

1 This manuscript is a **preprint** and has been submitted to the **Journal of Hydroinformatics**. Please
2 note that this manuscript is undergoing peer-review, and has not been accepted for publication.
3 Subsequent versions of this manuscript may have slightly different content. If accepted, the final
4 version of this manuscript will be available via the 'Peer-reviewed Publication DOI' link on the
5 right-hand side of this webpage. Please feel free to contact the corresponding author. We appreciate
6 your feedback.

7

8

9

10

11

12

13

14

15

16

17

18 **A Performance Comparison of Unsupervised Machine Learning Algorithms**
19 **for Clustering Water Depth Datasets at Urban Drainage Systems**

20 Jiada Li^{a*}, Simon Brewer^b

21 ^a Department of Civil and Environmental Engineering, University of Utah, 201 Presidents Circle,
22 Salt Lake City, UT 84112, USA

23 ^b Geography Department, University of Utah, 201 Presidents Circle, Salt Lake City, UT 84112,
24 USA

25 ^{a*} Corresponding author E-mail address: jiada.li@utah.edu

26

27 **Highlights**

28 1. Noise-free and -polluted water depth datasets of urban drainage systems are used for
29 clustering analysis.

30 2. The dendrogram cut-off point dominates the number of clusters in agglomerative clustering.

31 3. The number of clusters is found to be highly-related to sample length but is slightly relevant
32 to data magnitude.

33 4. Performance of K-means, Agglomerative, and Spectral clustering is assessed by three
34 metrics in grouping time-series water depth datasets.

35

36 **Abstract** As sensor measurements emerge in urban water systems, data-driven unsupervised
37 machine learning algorithms have been drawn tremendous interest in infrastructure monitoring,
38 flow prediction, and pollutant warning recently. However, most of them are applied in water
39 distribution systems, and few studies consider using unsupervised clustering analysis to group the
40 time-series hydraulic-hydrologic data at urban drainage systems. To improve the understanding of
41 how clustering analysis contributes to detecting urban flooding events, this study compared the
42 performance of K-means Clustering, Agglomerative Clustering, and Spectral Clustering in
43 uncovering time-series water depth similarity and finally identified the number of clusters with
44 maximum performance scores. In this work, the water depth datasets are simulated by a real-world
45 SWMM model and then formatted for a clustering problem. Three standard performance
46 evaluation scores, the SCI, CHI, and DBI, are employed to assess the clustering performance under
47 six artificial rainfalls and two recorded storms. The results indicate that SCI and DBI are
48 appropriate for assessing the performance of K-means Clustering and Agglomerative Clustering,
49 while CHI only works for Spectral Clustering. Noticeably, it was found that the number of clusters
50 is negatively related to the dataset length, but less correlated with the dataset magnitude.

51 **Keywords:** SWMM modeling, Unsupervised Machine Learning, Clustering analysis, Cluster
52 number, Data features

53

54

55

56

57 **1. Introduction**

58 Urban drainage systems (UDSs) are the infrastructures constructed to provide conveyance ability
59 and storage capability for surface inundation reduction, drainage overflow mitigation, and
60 pollutant removal. However, the existing UDSs, whose functionality can only serve for a limited
61 number of years, might degrade and even deteriorate as time goes by (Li *et al.* 2019). In recent
62 years, retrofitting the traditional UDSs with water-level sensors, velocity meters, and flow sensors
63 have been widely adopted as an adaptive and cost-effective solution for stormwater challenges
64 (Kerkez *et al.* 2016; Li *et al.* 2019). The deployed sensors can measure the water quantity and
65 quality data in a real-time way, which now makes it feasible for researchers and engineers to tap
66 into the UDSs. The need to understand the emerging data is crucial for forecasting extreme storms,
67 reducing sewer overflows, and predicting flash floods (Morales *et al.* 2017; Norbiato *et al.* 2008;
68 Wong & Kerkez 2016). Interpreting big water data into flood forecasting is attracting increasing
69 attention from researchers (Solomatine & Ostfeld, 2008; Henonin *et al.* 2013; Koo *et al.* 2015;
70 Vojinovic & Abbott 2017; Li *et al.* 2020).

71 In the last decade, many scholars have introduced a number of machine learning techniques to
72 investigate the available water resources and hydrological datasets (Diao *et al.* 2014; Hsu *et al.*
73 2013; Kang *et al.* 2013; Mullapudi & Kerkez 2018; Wang *et al.* 2009). Bowes *et al.* (2019)
74 compared long short-term memory and recurrent neural network by using a time-series of
75 groundwater table data in the city of Norfolk, Virginia. They explained that long short-term
76 memory is better than the recurrent neural network in predicting groundwater level, but takes about
77 three times longer to train the model. Hu *et al.* (2018) applied a boosted decision regression tree
78 to forecast flow with over 90% accuracy in combined sewer systems of Detroit city, Michigan.
79 Zhou *et al.* (2019) proposed an accurate deep learning algorithm to locate the pipe burst in water

80 distribution networks by using only 15 or 30 minutes of time-series pressure datasets collection.
81 However, the majority of these studies have focused on supervised learning (i.e., when a known
82 outcome is used to train the model), and unsupervised machine learning algorithms (UMLA) are
83 not commonly used in urban drainage systems.

84 Clustering analysis, one of the key unsupervised machine learning methods, has been applied in
85 many fields, including pattern recognition, image analysis, data compression, and anomaly
86 detection (Jain *et al.* 1999; Tan *et al.* 2005). In general, cluster analysis is based on identifying
87 similarities between observations. If a water quantity or quality event happens in the water system,
88 these observations are likely to be highly dissimilar to other observations (Wu *et al.* 2016). The
89 increase in dissimilarity would lead to these observations being considered as outliers, and thus
90 detected as anomalies. Although clustering analysis has been extensively discussed in municipal
91 topology classification and water distribution network simplification (Perelman & Ostfeld, 2012,
92 2011; Sela Perelman *et al.* 2015), the ability of UMLA methods to group time-series data at UDSs
93 is still unknown, and the most appropriate methods to assess these algorithms are unclear. Keogh
94 *et al.* (2003) concluded that clustering time-series data is meaningless, but this argument does not
95 cover the similarity-based clustering algorithms such as K-means and agglomerative clustering. In
96 contrast, Chen (2007, 2005) demonstrated that similarity-based cluster analysis could be
97 successfully applied to sequence datasets by using different distance measures. Wu *et al.* (2016)
98 adopted the clustering algorithm, developed by Rodriguez & Laio (2014), to detect the short-
99 duration pipe burst with a 0.61% false positive in water distribution systems. Xing & Sela (2019)
100 selected SC (Silhouette Coefficient) and CHI (Calinski-Harabasz Index) as the metrics to evaluate
101 K-mean Clustering (KC) performance in clustering time-series water pressure data and they finally
102 identified the number of clusters for the pressure sensor placement. However, it was unclear why

103 they chose these two indexes as the UMLA performance metrics. Previous studies from the
104 computer science field have demonstrated the differences and similarities among the popular
105 performance evaluation indexes such SH, CHI, and DBI (Aggarwal & Zhai 2012; Aranganayagi
106 & Thangavel, 2008; Celebi *et al.* 2013; Cordeiro De Amorim & Mirkin 2012; Xu & Tian 2015).
107 However, there is no systematic study of how these apply to time-series data from UDSs.

108 We can then define two questions, based on these previous research: 1) Which metrics are the most
109 suitable for assessing cluster model performance based on hydraulic-hydrologic data in UDSs; 2)
110 Which features of these time-series data (length, magnitude, and variability) are the most
111 influential for clustering analysis, and how does the choice of feature affect the clustering solution.
112 To answer these questions, it is necessary to explore how UMLA groups time-series water depth
113 data, and which assessment score can best represent UMLA performance. However, challenges for
114 implementing unsupervised learning algorithms to group the time-series data still exist. Firstly, it
115 is essential to re-format the time-series water depth datasets to make them suitable for clustering.
116 This difficulty is associated with the second research question above since the features of datasets
117 determine how we re-structure the data frame (Mosavi *et al.* 2018; Yaseen *et al.* 2019). Secondly,
118 the connection between the number of clusters and the clustering model performance is another
119 obstacle. As it is still unknown how to correlate clustering performance and the number of clusters
120 in the stormwater urban drainage field, it is required to build such a theoretical relationship for a
121 practical application like outlier detection (Fotovatikhah *et al.* 2018). Therefore, the objective of
122 this study is to improve the understanding of how UMLA facilitates detecting hydraulic anomaly
123 according to the characteristics of water depth datasets in urban drainage networks.

124 We hypothesize that the performance of clustering algorithms is related to the characteristics of
125 time-series hydraulic data. The layout of the study is as follows: 1) build KC, AC, and SC solutions

126 to group the time-series water depth data; 2) use UMLA metrics such as SCI (Silhouette
127 Coefficient Index), CHI (Calinski-Harabasz Index), and DBI (Davies-Bouldin Index) to evaluate
128 these solutions; 3) compare the best number of clusters obtained by each method; 4) investigate
129 the relationship between model performance and data characteristics. We start by describing the
130 implementation of different UMLA methods, followed by the research methodology with an
131 overview of the real-world case study, performance metrics, and simulation scenarios for cluster
132 analysis. Then we present the results and discussions and, finally, the conclusions.

133 **2. Description of Unsupervised Machine Learning Algorithms**

134 Current machine learning techniques mainly fall into two groups: supervised and unsupervised
135 learning (Kubat 2017). An unsupervised machine learning algorithm (UMLA) is a self-
136 organization method to find patterns in unlabeled data. Cluster analysis is, therefore, a subset of
137 UMLA methods, and in general, is based on the principle of grouping similar observations and
138 segmenting dissimilar observations (Xu & Wunsch 2005). Anomalous data points that differ from
139 others may then be filtered (Shannon 2007). A large number of clustering algorithms exist,
140 including K-means, Affinity Propagation, Mean Shift, DBSCAN, and HDBSCAN. In general, it
141 is difficult to recommend a single algorithm as being the most suitable for clustering, particularly
142 with data that is uncertain and of poor quality, such as the features of drainage data used here
143 (Maier *et al.* 2014; Solomatine and Ostfeld 2008). It is, therefore, advisable to use several
144 algorithms and compare their performance for specific applications. Here, we use K-means,
145 Spectral, and Agglomerative clustering to discover the unknown subgroups in simulated water
146 depth data of UDSs' junctions. Table 1 summarizes the advantages and disadvantages of these
147 algorithms.

Table 1 Clustering algorithm information summary

Models	Definition	Pros	Cons
K-means Clustering	A kind of vector quantization, partition data points into clusters by minimizing the intra-cluster distance.	1) fast, easy-to-understand, and wide applications; 2) stable for time-series data; 3) simple and efficient optimization performance; 4) suitable for huge datasets.	1) number of clusters; 2) spherical assumption.
Agglomerative Clustering	A kind of hierarchical clustering for merging clusters according to a measure of data dissimilarity.	1) stable runs 2) reasonable dendrogram cut-off nodes; 3) clusters growth without globular assumption; 4) good performance for time-series data; 5) no need to know the correct clusters' number.	1) number of clusters; 2) slow implementation; 3) cluster with polluted noise.
Spectral Clustering	A kind of graph clustering based on the distances between points.	1) stable due to the data transformation; 2) no purely globular cluster assumption; 3) easy to implement.	1) number of clusters; 2) slow performance; 3) cluster with polluted noise.

149

150 2.1 K-means Clustering

151 K-means Clustering (KC) is a centroid-based unsupervised clustering algorithm, originally
 152 designed for signal processing. It is the most widely applied method of cluster analysis in data
 153 mining (Celebi *et al.* 2013). K-means aims to partition the inputs into k partitions. Given a set of
 154 observations (x_1, x_2, \dots, x_i) for p variables, the algorithm runs as follows:

- 155 1) Choose k initial centroids, each defined by a value for each of the p variables. These are
 156 chosen randomly, often by simply choosing k observations.
- 157 2) Assign each observation to the centroid it is most similar to. The similarity is generally
 158 measured as the Euclidean distance between the observation and centroid in parameter
 159 space.
- 160 3) Once all observations are assigned, re-estimate the centroids location as the mean of the p
 161 variables of all observations assigned to that centroid.
- 162 4) Repeat until the algorithm stabilizes.

163 The goal then is to minimize kC_ℓ the within-cluster sum of squares:

$$164 \quad \operatorname{argmin}_{\mu, C} \sum_{\ell=1}^k \sum_{x_i \in C_\ell} \|x_i - \mu_\ell\|^2 \quad (1)$$

165 Where k is the number of cluster centers and $\{\mu_\ell\}, \ell = 1, \dots, k$ are the cluster centroids $C_\ell \mu_\ell \mu_\ell C_\ell$.
166 The total intra-cluster distance is the total squared Euclidean distance from each point to the center
167 of its cluster, and this is a measure of the variance or internal coherence of the clusters (Lloyd
168 1982). This can be used to assess the stability of the solution. When this falls below a predefined
169 threshold, the algorithm stops. The algorithm is often run multiple times with different random
170 starts to avoid problems in convergence. The clustering solution with the lowest sum-of-squares
171 is chosen as the final output.

172 However, the choice of k is challenging when model performance metrics are not available. Often,
173 an initial value of k is chosen, then the algorithm is repeated for higher and lower values. To
174 improve the efficiency of discovering the best k value, a scores-based performance assessment
175 method is recommended in many prior studies (Cordeiro De Amorim & Mirkin 2012).

176 **2.2 Agglomerative Clustering**

177 Agglomerative Clustering (AC) is one of the main forms of hierarchical clustering. These
178 algorithms do not provide a single partitioning of the data but instead provide a full hierarchy of
179 cluster solutions from all observations in a single cluster (i.e. $k=1$) to all observations in individual
180 clusters (i.e. $k=n$) (Rokach & Maimon 2010). In contrast to K-mean, hierarchical methods allow
181 existing clusters to be split or merged, with the result that smaller clusters are related to large
182 clusters in a hierarchy. The rules governing which clusters are again based on their distance or
183 similarity. The AC algorithm consists of the following steps:

- 184 1) Start with each data point as its own cluster.
- 185 2) Select the distance metric and linkage criteria to calculate the dissimilarity between pairs
186 of observations.
- 187 3) Link together the two clusters with the minimum dissimilarity.
- 188 4) Continue this process until there is only one cluster.

189 A key decision in the AC algorithm is the calculation of dissimilarity between clusters. In this
190 study, we used Euclidean distance (Danielsson 1980), and the Ward linkage, which measures the
191 distance between the cluster centroids, similar to the K-means clustering method (Ward 1963).
192 The equations for Euclidean distance and Ward linkage are defined by equation (2) and (3),
193 respectively:

194
$$\|a - b\|_2 = \sqrt{\sum_i (a_i - b_i)^2} \quad (2)$$

195 Where a and b mean the Euclidean vector; a_i and b_i are the point position for the Euclidean vector;
196 i is the number of vectors.

197
$$d_{ij} = d(\{X_i\}, \{X_j\}) = \|X_i - X_j\|^2 \quad (3)$$

198 Where d_{ij} is the squared Euclidean distance between point i and point j; X_i and X_j are Ward's
199 vectors.

200 The resulting hierarchy of clusters can be represented using a dendrogram plot (Forina *et al.*
201 2002). In a dendrogram plot, the y-axis marks the distance at which the clusters merge, while the
202 observations are arranged along the x-axis according to their cluster membership. The dendrogram

203 can then be “cut” at any height on the y-axis to obtain a required number of clusters, with lower
204 heights giving a larger number.

205 **2.3 Spectral Clustering**

206 Spectral Clustering (SC) is an unsupervised learning technique based on graph theory, where SC
207 takes advantage of graph information from the spectrum to find the number of clusters (Von
208 Luxburg 2007). Unlike the previous methods that tend to prioritize clusters by proximity, SC aims
209 to identify observations that are linked, and therefore may not form classical spherical groups in
210 parameter space (Hastie *et al.* 2009). The SC algorithm is as follows:

211 1) Create a similarity matrix S between observations. This is the complement to the
212 dissimilarity matrices used in other methods, and here is calculated as the negative
213 Euclidean distance.

214 2) Create an adjacency matrix A , representing the graph or connectivity between observations.
215 This is a transformation of S , where for each observation, we find the k nearest neighbors
216 (i.e., with the highest similarity). If observations i and j are considered to be neighbors, we
217 set $A_{ij} = S_{ij}$. If not, we set $A_{ij} = 0$.

218 3) Create a degree matrix D , where the diagonal values are the degree of connectivity for each
219 observation, given as $\text{diag}\{D\} = \sum_{i,j}^n A_{ij}$, $i,j=1,2,3,\dots,n$

220 4) Next, calculate the graph Laplacian. This can be normalized or unnormalized. Here, we
221 use the unnormalized: $L = D - A$

222 5) The clustering solution is then found by eigendecomposition of the Laplacian, and selecting
223 the k smallest eigenvectors. Consequently, these result in a perfect separation of the

224 observations. K-means is then run on these eigenvectors, to get the final cluster assignment
225 of each observation: $L_{(N \times N)} = D - A$

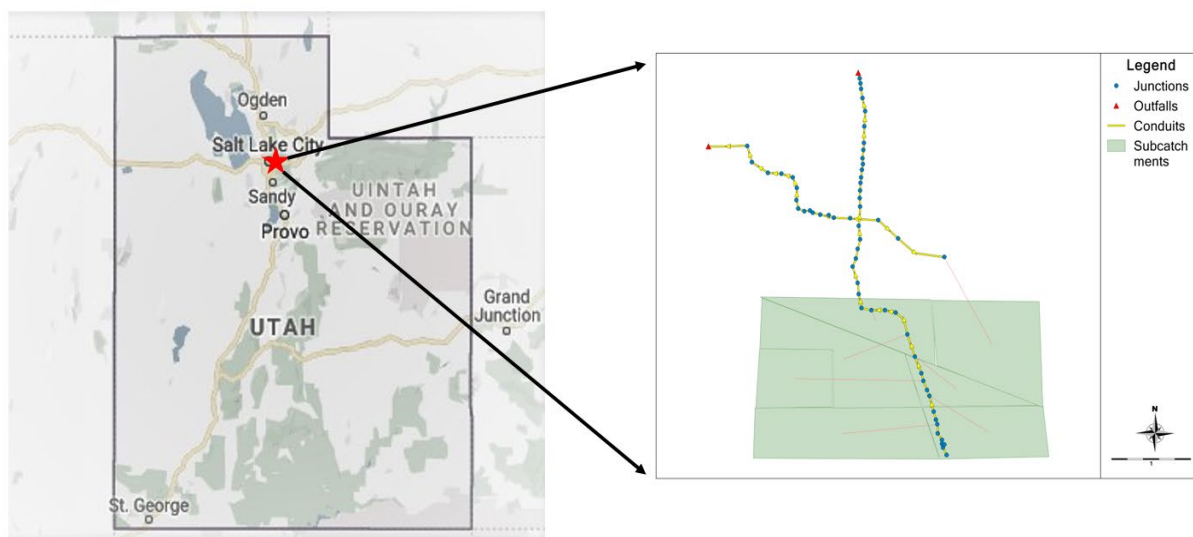
226 As SC performs dimensionality reduction before clustering data points, it is a very flexible
227 approach for complex data sets. However, the similarity matrix generated by SC may include
228 negative values, which can be problematic for grouping time-series points (Zhang *et al.* 2008).

229 **3. Methods**

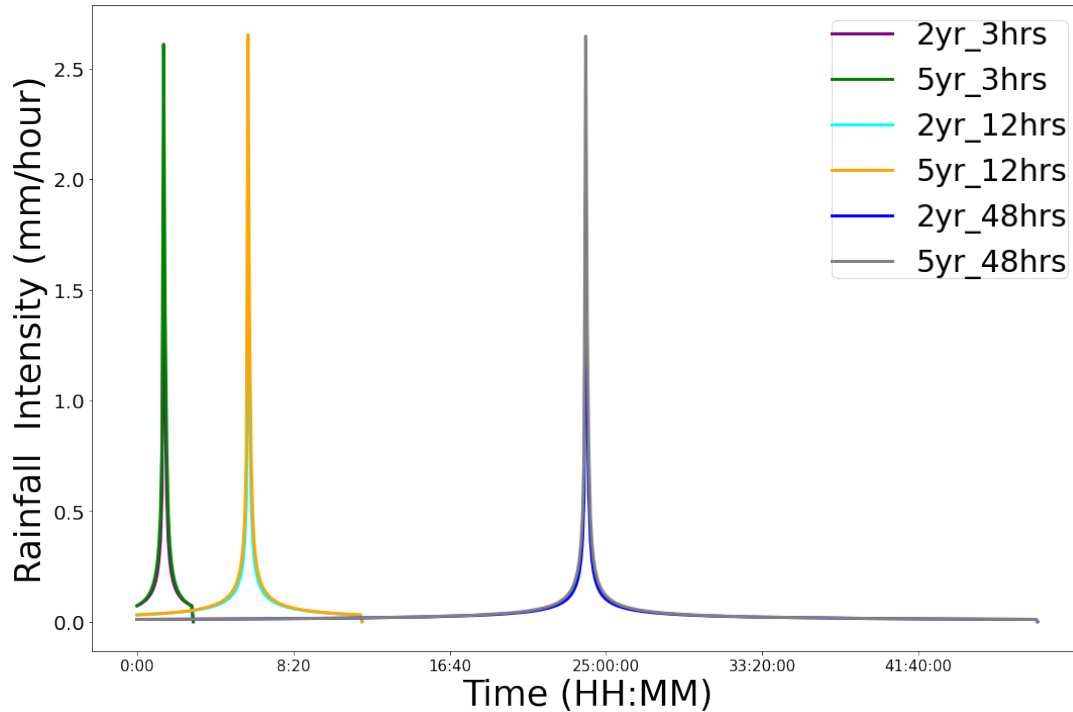
230 **3.1 Study Area and Data Description**

231 A real-world urban drainage system located in Salt Lake City, Utah, the U.S., was selected as the
232 case study. Due to climate change and urbanization, the studied area has suffered from floods more
233 frequently than before, and the increase in the magnitude and duration of the storm events has
234 pushed the resulting urban drainage out of the pre-defined performance level. Particularly, the
235 flash flooding event on July 26, 2017, which caused millions of dollars of economic loss, was
236 estimated as a 200-year return period storm. This urban drainage network was represented by a
237 rainfall-runoff SWMM (Storm Water Management Model) model. SWMM, which is used
238 throughout the world for planning, analysis, and design related to stormwater runoff, combined
239 and sanitary sewers, and other drainage systems, is a state-of-art tool developed to help support
240 local, state, and national stormwater management objectives to reduce runoff, discharge, and
241 improve stormwater quality (Rossman 2015). Figure.1 shows the components of this SWMM
242 model, which includes one rain gauge, 60 junctions, 61 conduits, two outfalls, and seven sub-
243 catchments.

244 A total number of 6 artificially designed rainfalls generated by using PCSWMM 7.3 are imported
245 into SWMM as model inputs. Artificial rainfall events are used to test the clustering algorithms as
246 these allow us to control the input and reduce the possible sources of variation between the
247 algorithm results. PCSWMM has its approaches, such as Chicago distribution and SCS distribution,
248 to design rainfall patterns based on precipitation records. For this study, however, we created
249 artificial precipitation series externally and imported them into SWMM within the PCSWMM
250 interface. The distribution for the synthetic rains is shown in Figure.2. These rainfalls have
251 durations of 3 hours, 12 hours, to 48 hours. The return period ranges from 2-year to 5-year.
252 Additionally, rainfall measurements for two real rainfall events were collected to test the clustering
253 algorithm. These rain records are from 2015/05/05 rainfall (3-hour duration) and 2015/07/08 (24-
254 hour duration) rainfall with variable rainfall duration, volume, and intensity. Compared with water
255 depth generated by the artificially designed rainfall data, the time-series water depth produced by
256 the real-world storms is more close to field datasets with non-stationarity and noise.



257
258 Figure.1. Study area located in the northern Utah state, the U.S. (left subplot: red star), and the topological view of the
259 urban drainage system model plotted by PCSWMM 7.2 (right subplot: scale unit is kilometer).



260

261 Figure.2. Distribution plots of artificially designed rainfalls with different return periods and rainfall duration, where
 262 ‘yr’ represents the year and ‘hrs’ stands for hours.

263 **3.2 Clustering Model Implementation**

264 The SWMM model was run six times, once with each of the rainfall scenarios described above.
 265 We collected the simulated time-series water depth from each node in the drainage network for
 266 cluster analysis. As there are 60 junctions in the SWMM model, this results in a matrix where each
 267 column represents a single time step with a 5-minute interval, and each row stands for a junction
 268 or node in the network. We then used the principal component analysis (PCA) to reduce the
 269 dimensionality of this matrix. PCA uses the eigendecomposition of the correlation matrix to
 270 identify a small set of principal components that represent the majority of variance in the original
 271 data (Bro and Smilde 2014). Here, we used correlations between the time-series at different nodes
 272 to reduce the data from 60 rows to 2. While other techniques for data reduction exist (e.g.,
 273 correspondence analysis (CCA), factor analysis (FA), or non-metric multi-dimensional scaling

274 (NMDS)), we used PCA due to the assumed linear response of the water depth values. Although
275 the reduction of dimensionality might cause data loss or an undesirable relationship between axes,
276 it is true that PCA helps reduce computation time and remove redundant data features in the
277 following clustering analysis.

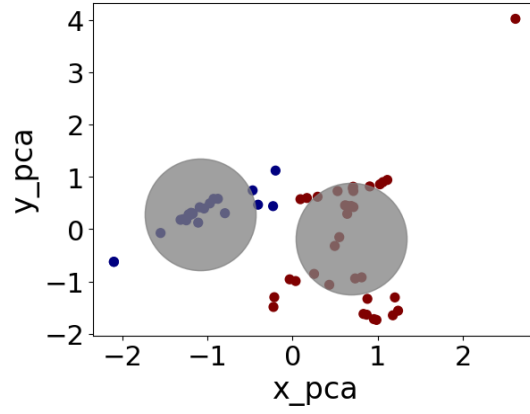
278 All clustering algorithms were then run using this set of two principal components, with the
279 following set up:

280 1) K-means: we initially set the number of clusters (k) to 2 for each modeling scenarios, as
281 shown in Figure 2. The algorithm was repeated ten times with different random
282 initialization, and a maximum of 5 iterations was used to converge the algorithm.

283 2) Agglomerative clustering model: we used Ward linkage, as this is robust to outliers and
284 unequal variance in the data. As only 'Euclidean' supports 'Ward' linkage distance
285 computation. If 'Ward' linkage is used for cluster distance computation, 'Euclidean' would
286 be the best way to measure the data dissimilarity (Pedregosa *et al.* 2011). Thus, the cluster
287 distance calculation method and dissimilarity metric among sample points are set to be
288 'Ward' and 'Euclidean' distance, respectively. The resulting hierarchy was cut to provide
289 2 clusters.

290 3) Spectral clustering: the algorithm was used to identify 2 clusters, using the unnormalized
291 graph Laplacian

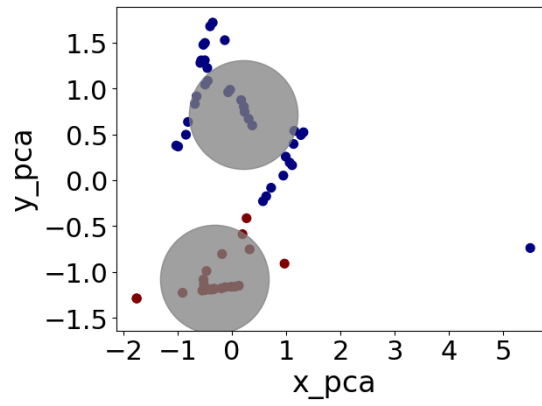
292



293

294

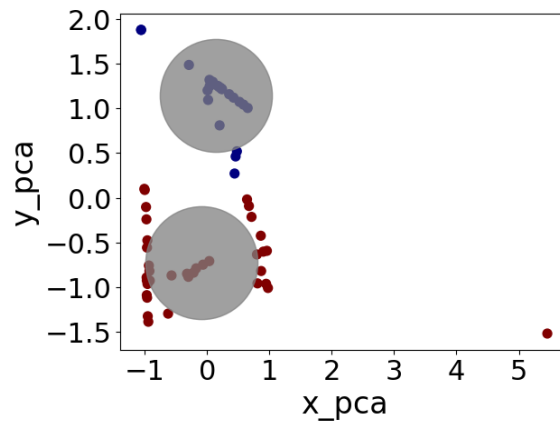
(a)



295

296

(b)



297

298

(c)

299 Figure.3 Datasets (x_pca means the first dimension datasets after principal component analysis; y_pca means the
300 second dimension datasets after principal component analysis) partition by K-mean clustering with 2 clusters (gray
301 circles) under varying rainfall scenarios: a) 3 hours duration rainfall, b) 12 hours duration rainfall, c) 48 hours duration
302 rainfall.

303 **3.3 Clustering Model Evaluation and Validation**

304 Unlike the supervised machine learning algorithm, which can compare the predicted values with
305 the actual values to obtain a measure of model accuracy, UMLA has to assess performance directly
306 on the characteristics of the clusters that were obtained. The performance then depends on data
307 features selected, data preprocessing and parameter settings such as the distance function to use, a
308 density threshold, or the number of expected clusters, which can be modified according to the
309 varying datasets and object inputs. As a result, there is rarely a single obvious solution for clusters,
310 and CA is an iterative process of knowledge discovery or interactive multi-objective optimization
311 that involves trial and failure, aimed to obtain the desired results (Maulik & Bandyopadhyay 2002).
312 Several indices have been proposed to measure the relative performance of different clustering
313 algorithms. In general, these provide an assessment of how the data variance is partitioned. An
314 ideal cluster solution will have low intra-cluster variance (i.e., all observations should be similar
315 within a cluster) and high inter-cluster variance (the clusters should be well separated). Three of
316 these indices are widely used: Silhouette Coefficient (SC), Calinski-Harabasz Index (CHI), and
317 Davies-Bouldin Index (DBI) (Al-Zoubi and Al Rawi 2008; Maulik and Bandyopadhyay 2002;
318 Xiao *et al.* 2017), due to their accuracy and reliability, and we used these here to assess our results.

319 **3.3.1 Silhouette Coefficient Index**

320 The Silhouette Coefficient Index (SCI) is an example of model-self evaluation, where a higher SCI
321 score relates to a model with better-defined clusters (Al-Zoubi & Al Rawi 2008). This score is

322 bounded between -1 for incorrect clustering and +1 for well-formed clusters. Scores around zero
323 indicate overlapping clusters. The SCI is defined for each observation, which can be calculated as
324 equation (5):

$$325 \quad s = \frac{m-n}{\max(m,n)} \quad (5)$$

326 Where the s is SCI for a single observation; m is the mean distance between an observation and
327 all other observations in the same class; n is the mean distance between the same observation and
328 all observations in the next nearest cluster. The SCI has the advantage that it can be used to
329 examine how well individual observations are clustered, or an estimate can be obtained for each
330 cluster or for the whole cluster solution by averaging across a cluster or the entire dataset,
331 respectively. An estimate can be obtained for each cluster or for the whole clusters solution; a set
332 of samples is given as the mean of the SCI for each sample, and it would be relatively higher when
333 clusters are dense and well separated (Aranganayagi & Thangavel 2008).

334 **3.3.2 Calinski-Harabasz Index**

335 The CHI (also known as the Variance Ratio Criterion) is calculated as the ratio of the between-
336 clusters dispersion average and the within-cluster dispersion (Caliński & Harabasz, 1974),
337 penalized by the number of clusters (k). A higher CHI score indicates better-defined clusters (i.e.,
338 dense and well separated). CHI for a set of k clusters is calculated as:

$$339 \quad s(k) = \frac{T_r(B_k)}{T_r(W_k)} \times \frac{N-k}{k-1} \quad (6)$$

340 Where N is the number of points in our data; k is the number of the cluster; T_r represents
 341 dispersion matrix; B_k is the between-group dispersion matrix, and W_k is the within-cluster
 342 dispersion matrix. B_k and W_k are defined by the following equations:

$$343 \quad W_k = \sum_{q=1}^k \sum_{x \in C_q} (x - c_q)(x - c_q)^T \quad (7)$$

$$344 \quad B_k = \sum_q^k n_q (c_q - c)(c_q - c)^T \quad (8)$$

345 Where C_q is the set of points in the cluster q , c_q is the center of the cluster q , c is the center of the
 346 whole data set which has been clustered into k clusters, n_q is the number of points in the cluster q .

347 **3.3.3 Davies-Bouldin Index**

348 Davies-Bouldin Index (DBI) can also be used to evaluate the model, where a lower DBI relates to
 349 a model with better separation between the clusters (Davies & Bouldin 1979). The index is defined
 350 as the average similarity (R_{ij}) between each cluster and the next closest (i.e., most similar) cluster.
 351 The DBI is calculated as equation (9):

$$352 \quad DB = \frac{1}{k} \sum_{i=1}^k \max_{i \neq j} (R_{ij}) \quad (9)$$

353 Where DB is the Davies-Bouldin index; Zero is the lowest possible score. Values closer to zero
 354 indicate a better partition. k is the number of the cluster; R_{ij} is the similarity measure which
 355 features as equation (10):

$$356 \quad R_{ij} = \frac{s_i + s_j}{d_{ij}} \quad (10)$$

357 Where s_i is the average intra-distance between each point of cluster i and the centroid of that
 358 cluster representing as cluster diameter; d_{ij} is the inter-cluster distance between cluster centroids
 359 i and j ; R_{ij} is set to the trade-off between inter-cluster distance and intra-cluster distance. The
 360 computation of DBI is simpler than that of SC since this index is computed only with quantities
 361 and features inherent to the dataset (Petrovic 2006). However, a good value reported by DBI might
 362 not imply the best information retrieval (Xiao *et al.* 2017).

363 3.3.4 Intra-Cluster Distance

364 Intra-cluster distance is the distance between two samples belonging to the same cluster. Three
 365 types of intra-cluster distance, including complete diameter distance, average diameter distance,
 366 and centroid diameter distance, are popular in prior studies. As the number of clusters increase,
 367 individual clusters become more homogenous, and the intra-cluster distance decreases. At a certain
 368 point, the decrease in distances becomes negligible. Plotting this distance against k usually results
 369 in an inflection point or elbow where this occurs, and can be used to identify the optimal value of
 370 k (Thorndike 1953). The number of clusters is chosen at this point, hence the "elbow criterion."
 371 Here we use the centroid distance to represent intra-cluster distance, given as double the average
 372 distance between all of the objects:

$$373 \quad \Delta(S) = 2 \left\{ \frac{\sum_{x \in S} d(x, T)}{|S|} \right\} \quad (11)$$

$$374 \quad T = \frac{1}{|S|} \sum_{x \in S} x \quad (12)$$

375 Where $\Delta(S)$ is the centroid diameter distance of the formed cluster representative S ; x is the
 376 samples belonging to cluster S ; $d(x, T)$ is the distance between two objects, x , and T ; $|S|$ is the
 377 number of objects in cluster S .

378 3.3.5 Dendrogram

379 A dendrogram is a visualization in the form of a tree that shows the hierarchical relationship like
380 the order and distance (dissimilarity) between samples (Stanford 2012). The individual samples
381 are located along the bottom of the dendrogram and referred to leaf nodes. The hierarchical clusters
382 are formed by merging individual samples or existing lower-level clusters. In a dendrogram, the
383 vertical axis is labeled distance and refers to a dissimilarity measure between individual samples
384 or clusters. Generally, in a dendrogram, horizontal lines can be regarded as places where clusters
385 merge, while vertical lines show the distance at which lower-level clusters were merged, forming
386 a new higher-level cluster. The dissimilarity measure between two groups is calculated as equation
387 (13):

$$388 \qquad \qquad \qquad \text{Dis} = 1 - C \qquad \qquad \qquad (13)$$

389 where Dis means the Dissimilarity or Distance among objects; C means the correlation degree
390 between clusters.

391 If clusters are highly correlated to each other, they will have a correlation value close to 1. To that,
392 $\text{Dis} = 1 - C$ will be given a value close to zero. Therefore, highly related clusters are nearer to the
393 bottom of the dendrogram. Those clusters that are not correlated have a correlation value close to
394 zero. Clusters that are negatively correlated will give a distance value larger than 1 in the
395 dendrogram. The dendrogram can be used to visually allocate correlated objects to clusters or to
396 detect outliers and anomaly in a diagram (Forina *et al.* 2002). In the dendrogram, each sample is
397 treated as a single cluster and then successively combines pairs of clusters until all clusters have
398 been merged into a single cluster. In this process, the dendrogram shows how the aggregations are
399 performed from bottom to top tree statically. This procedure allows the cut-off points to flexibly

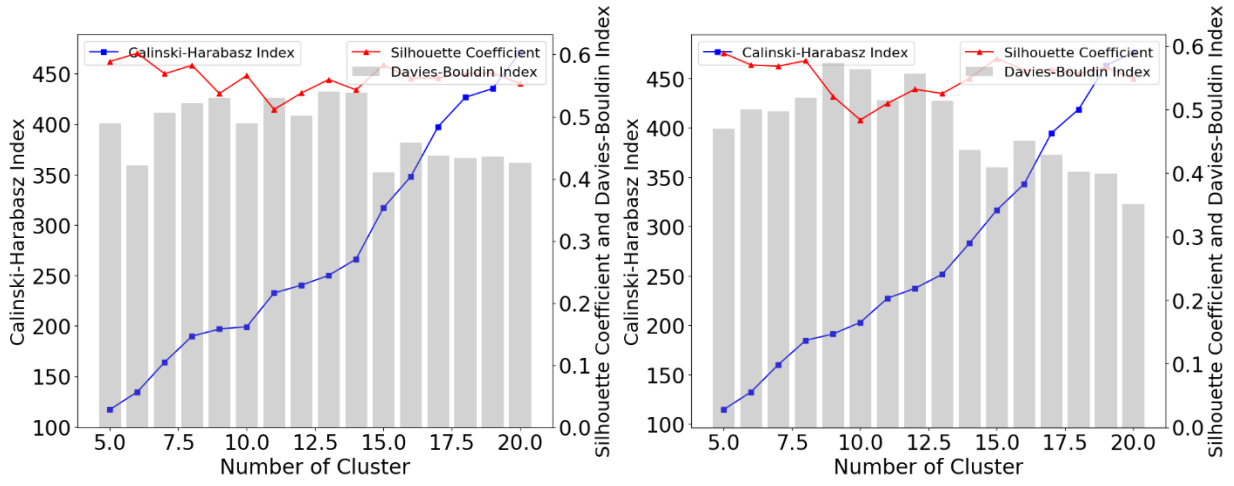
400 and efficiently represent the number of clusters. Therefore, this study used the number of cut-off
401 points in the dendrogram to validate the cluster number of the agglomerative clustering.

402 **4. Results**

403 **4.1 Clustering Performance Evaluation**

404 Figure 4 shows how three performance metrics SCI (Silhouette Coefficient Index), CHI (Calinski-
405 Harabasz Index), and DBI (Davies-Bouldin Index) change with different cluster numbers when
406 using K-means to cluster the time-series water depth data. Values for the CHI value increase with
407 higher cluster numbers, whereas the SCI and BDI values fluctuate. The SCI and DBI values show
408 opposite trends, reflecting the different methods by which they are calculated (see above). In
409 particular, Figure.4 b and c show that the best solution is with 8 clusters, reflected in the largest
410 SC value and smallest DBI value. These results suggest that the SCI and DBI are more suitable to
411 assess the performance of K-means, while any peak in the CHI related to cluster quality is eclipsed
412 by the influence of increasing the number of clusters. Based on the SCI and DBI value in Figure.4a,
413 the optimal number of clusters is 6 for the 2year-3hour and 5year-3hour rainfall scenarios. The
414 differences in the optimal number of clusters among Figure.4 a, b, and c indicate that rainfall
415 duration has impacts on the number of clusters when utilizing KC to group time-series water depth
416 datasets.

417

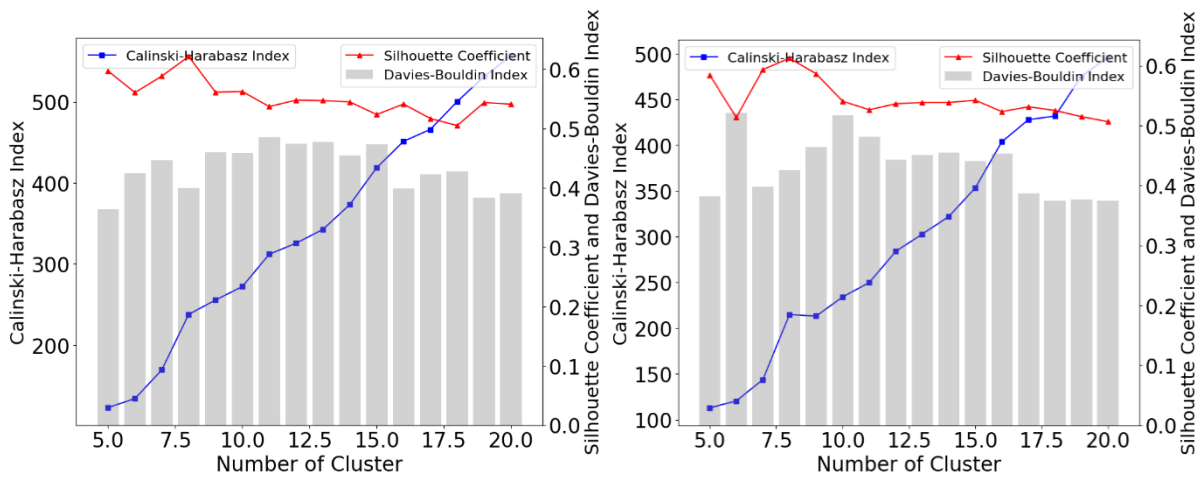


418

419

420

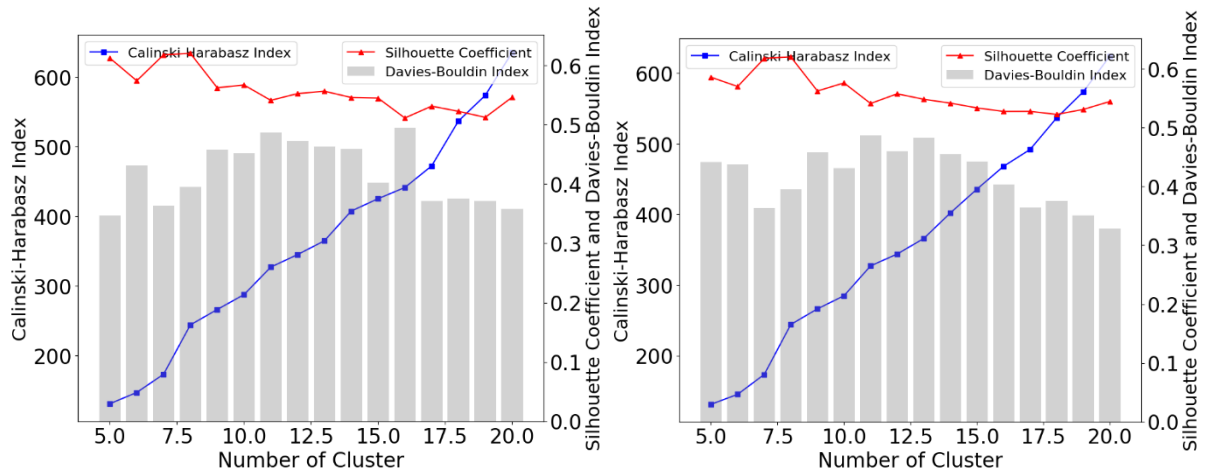
(a)



421

422

(b)



423

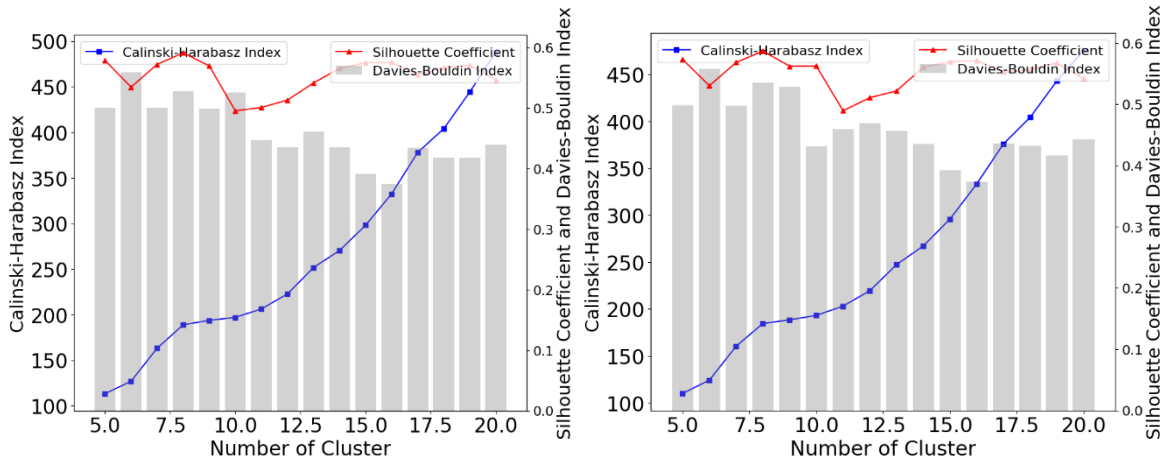
424

(c)

425 Figure.4. Performance evaluation for K-means Clustering with different cluster numbers under synthetic rainfall
 426 scenarios including a) 3-hour (2-year and 5-year), b) 12-hour (2-year and 5-year), and c) 48-hour duration (2-year and
 427 5-year).

428 Figure 5 shows the same results but based on the use of Agglomerative Clustering to group the
 429 time-series water depth data. As with the K-means results (figure 4), the CHI value increase with
 430 the number of clusters for all scenarios from short-duration to long-duration rainfall. Again, it is
 431 difficult to identify any peak representing an optimal number of clusters, and this suggests that the
 432 CHI is not suitable for ascertaining the best clustering solution with these data. In contrast, the SCI
 433 and DBI show clear peaks in their values. Figure.5a shows that 16 clusters result in the maximum
 434 SCI close to 0.76 and minimum DBI with 0.38. Figure.5c shows a peak in SCI values (~ 0.6) for 8
 435 clusters, with a corresponding minimum in the DBI value (< 0.4). However, Figure.5b shows that
 436 8 clusters could produce the largest SCI (~ 0.62) and the lowest DBI (~ 0.40) with the 2year-12hour
 437 rainfall duration scenario (left subplot), but that 16 clusters are the optimal solution for the 2yr-
 438 12hour rainfall (SCI ~ 0.58 and DBI ~ 0.38 ; right subplot). In summary, the best cluster solutions
 439 AC algorithms are 16, 8, and 8 under 3 hours, 12 hours, and 48-hour duration rainfalls, respectively.

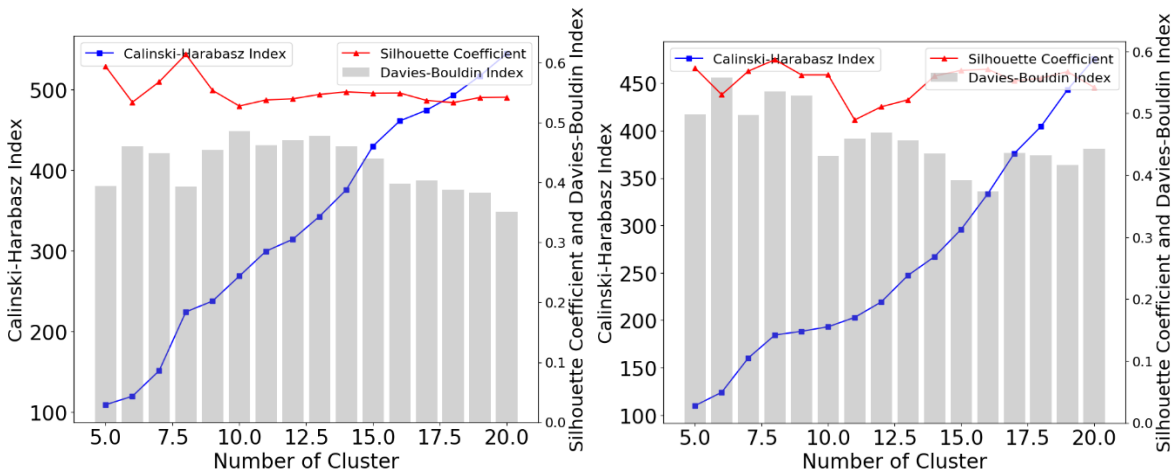
440 Comparing the left subplots with the right subplots provides (Figure.5) evidence that the cluster
 441 number for the best AC performance remains the same, although the return period has been shifted
 442 from 2-year to 5-year. The rainfall return period (annual exceedance probability) was found to be
 443 less related to the number of clusters.



444

445

(a)



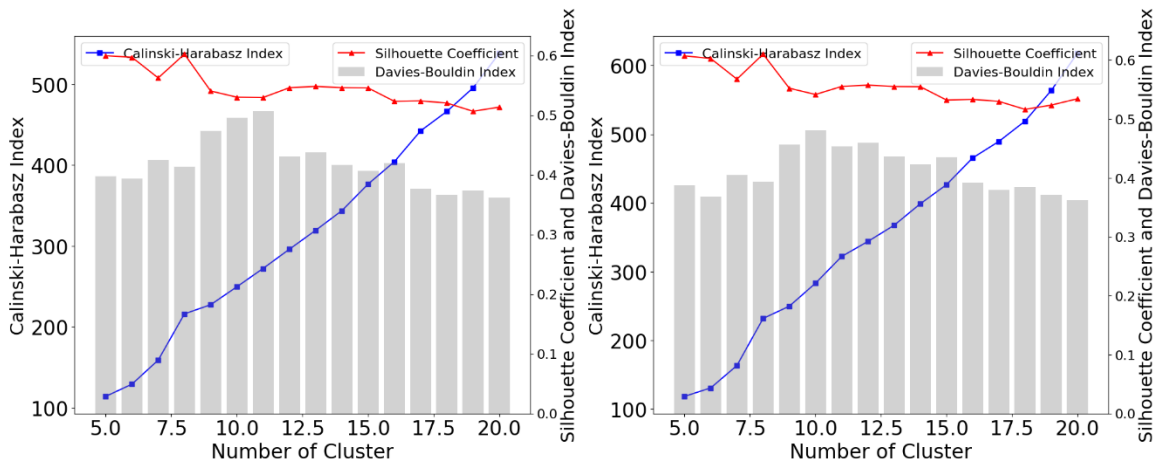
446

447

448

(b)

449



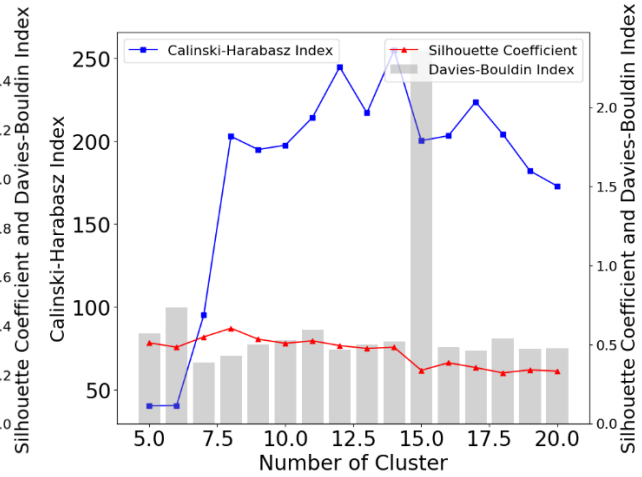
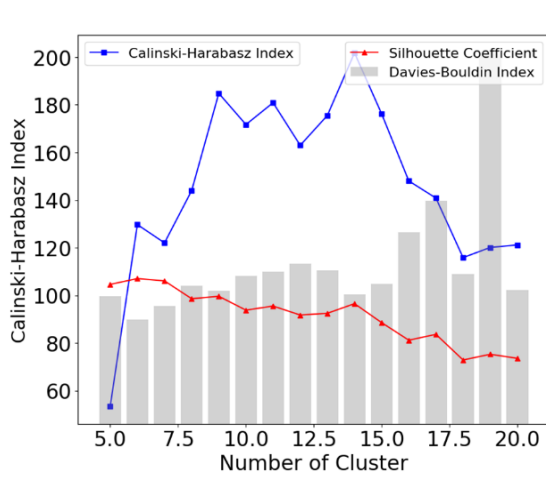
450

451

(c)

452 Figure.5. Performance evaluation for Agglomerative Clustering with different cluster numbers under synthetic rainfall
 453 scenarios including a) 3-hour (2-year and 5-year), b) 12-hour (2-year and 5-year), and c) 48-hour duration (2-year and
 454 5-year).

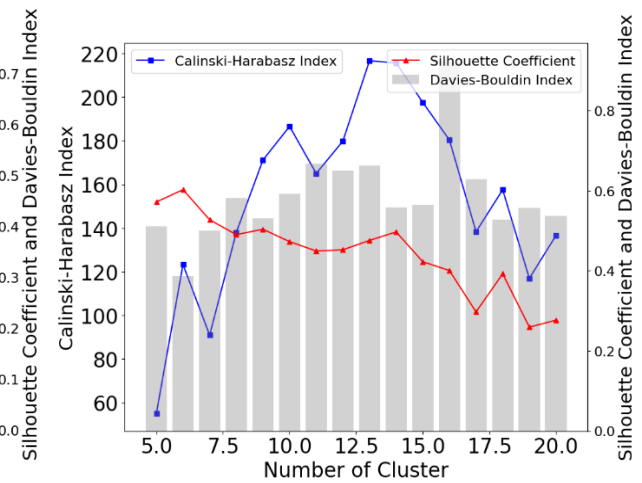
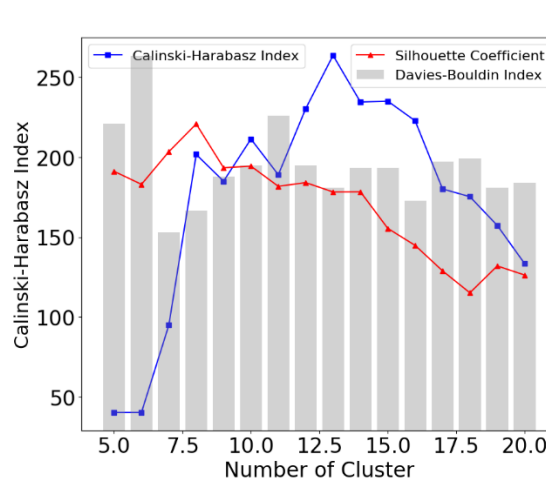
455 Figure. 6 shows the results obtained for different cluster numbers using Spectral Clustering to
 456 group the time-series water depth data. In contrast to the two previous methods, the SCI values
 457 decrease as the number of clusters increase. For the 12 and 48 hour scenarios, this index identifies
 458 solutions at about 6 to 7 clusters, but no clear optimal solution is identified in the shorter scenarios
 459 (panel a). This suggests that this index is unsuitable for assessing this algorithm. The DBI values
 460 show greater variation as the number of clusters change, although minima can be observed at 6 to
 461 7 clusters for most scenarios. The CHI values no longer show a linear increase, but show clear
 462 peaks, although usually for higher numbers of clusters than the DBI identifies. The highest CHI
 463 values (275 for 2 year-12hours and 190 for 5 year-12hours) are all generated by the SC with 13
 464 clusters. For the for 2 year-48 hours and 5 year-48 hours scenarios, the largest CHI values are
 465 approximately 200 and 270, respectively, in both cases for 12 clusters.



466

467

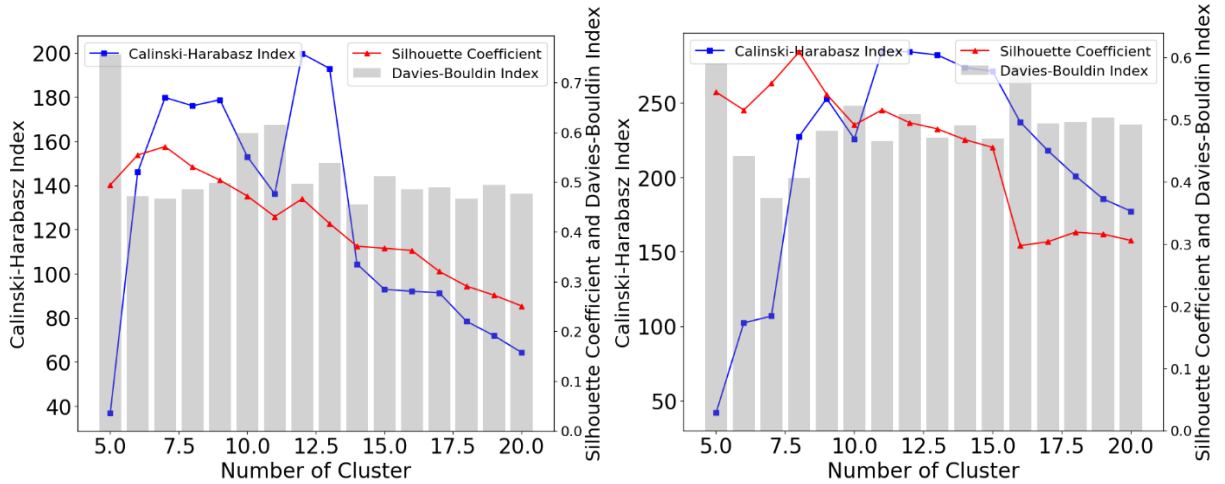
(a)



468

469

(b)



470

471

(c)

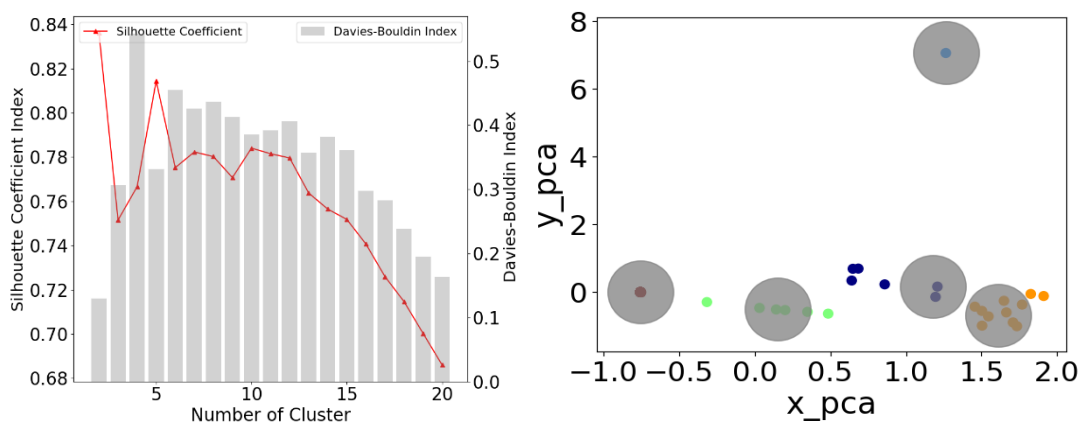
472 Figure.6. Performance evaluation for Spectral Clustering with different cluster numbers under synthetic rainfall
 473 scenarios including a) 3-hour (2-year and 5-year), b) 12-hour (2-year and 5-year), and c) 48-hour duration (2-year and
 474 5-year).

475 4.2 Clustering Performance Testing

476 The analysis of cluster performance in the previous section is based on synthetic rainfall datasets,
 477 due to the shortage of sensor monitoring for water depth in manholes. However, the use of noise-
 478 free synthetic data may have a significant impact on the results obtained (Moazenzadeh *et al.* 2018;
 479 Mosavi *et al.* 2018), and our results may not represent real storm situations or currently changing
 480 climate conditions. To validate that the results obtained from designed rainfalls can also be applied
 481 to non-stationary real-storms, we further investigated the performance of the clustering analysis in
 482 grouping water depth datasets generated by two complete rainfall events described below.

483 The left plots in Figure.7 indicate that the best number of clusters for 2015/05/05 rainfall (Figure
 484 7.a), and 2015/07/08 rainfall (Figure 7.b) are 5 and 4, respectively. Increasing the number of
 485 clusters beyond this causes both the SCI and the DBI to decline. The distribution of different

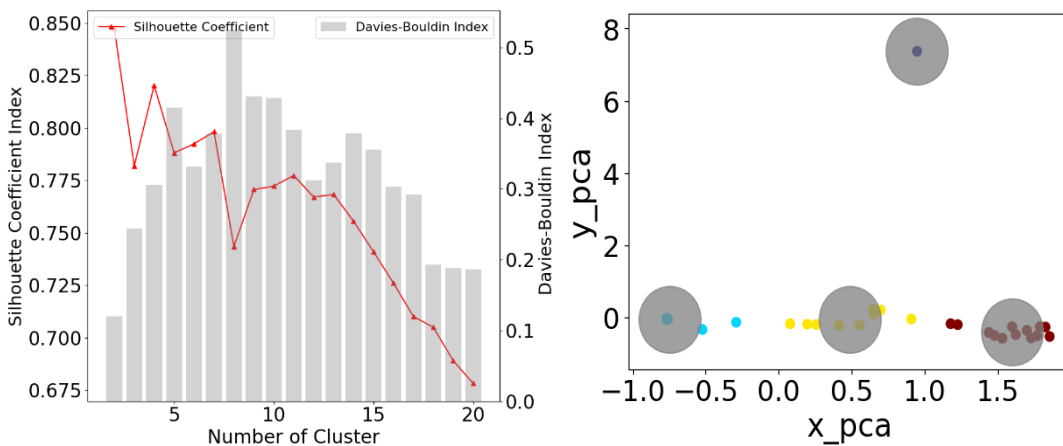
486 clusters obtained is shown in the PCA plots in the right panel of Figure .7. These show that the
 487 cluster analysis resulted in a good separation of the storm events (indicated by the lack of overlap
 488 between the gray circles). As the rainfall duration increases from 3 hours (the 2015/05/05 storm)
 489 to 24 hours (the 2015/07/08 storm), the reduction in the number of clusters selected is in line with
 490 the results in section 4, supporting the negative correlation between the number of cluster and
 491 rainfall duration.



492

493

(a)



494

495

(b)

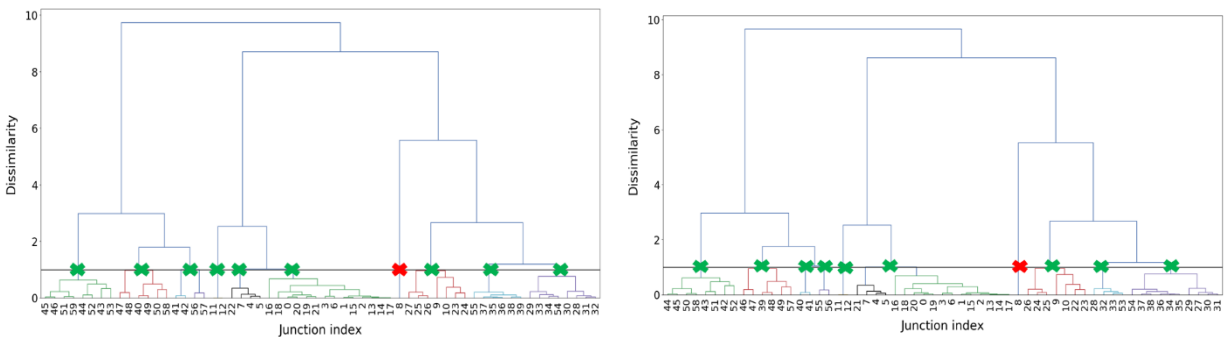
496 Figure .7 Clustering analysis test for time-series water depth generated by a) 2015-05-05 storm event; b) 2015-07-08
497 storm event (gray circles same to clusters).

498 **4.3 Cluster Number Validation**

499 Figure.8 shows the dendrogram plots obtained from applying the Agglomerative Clustering
500 algorithm to the observed rainfall data. Generally, the cut-off point should be at least 70%
501 dissimilarity between two clusters or cutting where the dendrogram difference is most significant
502 (Suzuki and Shimodaira 2013). The number of clusters was selected by using a distance threshold
503 of 0.9 distance or 90% dissimilarity, and this is plotted as a horizontal cut-off line in all
504 dendrograms of Figure.8. The cross points (highlighted as green X in dendrogram) between the
505 cut-off line and dendrogram leaves identify the accepted clusters. In Figure.8, one point identified
506 by the cut-off line (junction 8; highlighted as red X in dendrogram) was considered as an outlier
507 in the dendrogram and excluded. In practice, this algorithm might be helpful for anomaly detection
508 in the sensor monitoring network. For instance, real-time monitoring is built to capture the varying
509 different features of measurements as much as possible within a limited number of sensors
510 (Sambito *et al.* 2019). Further, the clusters represent different parts of the hydrological network
511 and can be used to help target locations for sensor deployment to observe overflow and flooding
512 events in the field.

513 The vertical comparisons among the subplots of Figure.8 (a, b, c) disclosed that the appropriate
514 cluster numbers for 3 hours, 12 hours, and 48 hours rainfall scenarios are quite similar; 8, 9, and
515 9, respectively. Meanwhile, comparing cluster solutions for different time periods (e.g., left and
516 right plot of Figure.8a), the number of clusters and their structure is remarkably similar, implying
517 that the rainfall return period has fewer impacts on AC model performance. This supports the

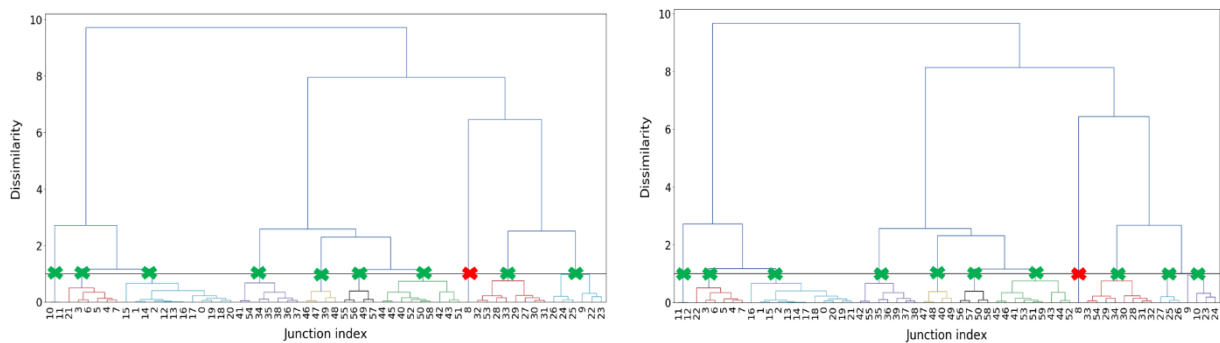
518 conclusions reached with the synthetic time series, that the AC model performance noticeably
519 depends on the rainfall duration but not the rainfall return period (exceedance probability).



520

521

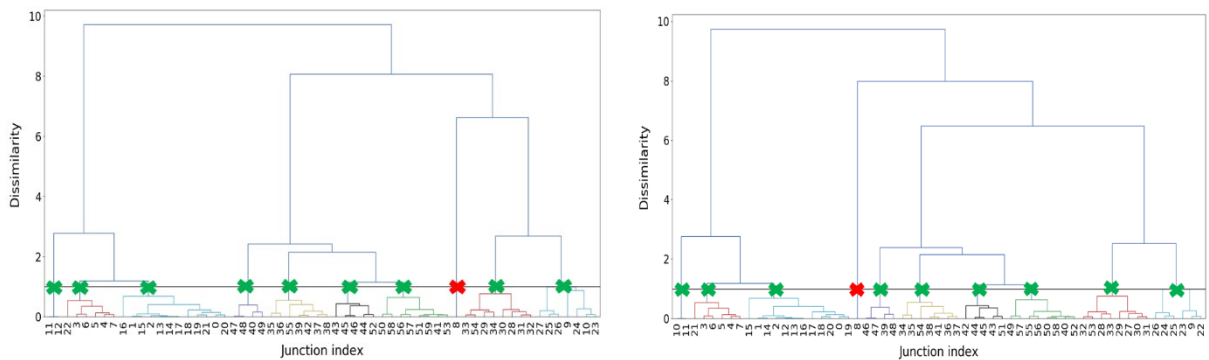
(a: left 2year-3hours; right 5year-3hours)



522

523

(b: left 2year-12hours; right 5year-12hours)



524

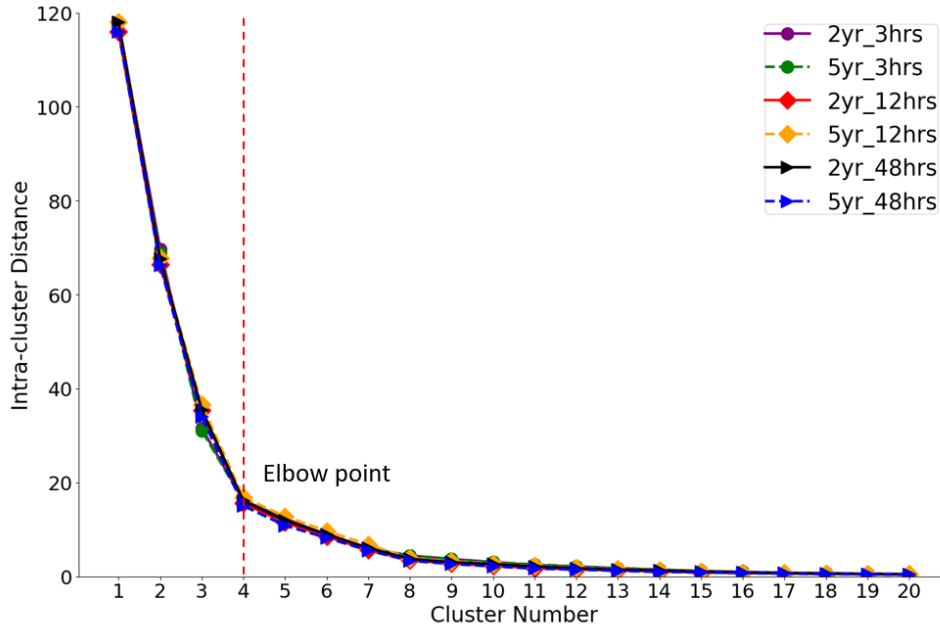
525

(c: left 2year-48hours; right 5year-48hours)

526 Figure.8 Dendrogram (green X representing acceptable cluster; red X representing unacceptable X) for comparing
527 agglomerative cluster numbers between 2-year return period (the left subplots) and 5-year return period (the right
528 subplots) rainfall scenarios.

529 This study adopted intra-cluster distance as the metric to assess the effects of rainfall duration and
530 return period (exceedance probability) on the performance of the K-means and Spectral Clustering
531 algorithm. Figure.9 shows the results of this comparison, with the decay in the intra-cluster
532 distance as the number of clusters increases. A notable elbow can be seen above 4 clusters, as the
533 decrease in distances becomes much smaller. Using the elbow criterion described in section 3.3.4,
534 this suggests that 4 clusters are the best solution. Increasing the number of clusters beyond this
535 would result in a little additional gain for the extra complexity of the solution. Figure.9 shows that
536 the intra-cluster distance changes in a similar way for all six rainfall scenarios, and that the intra-
537 cluster distance is identical in those rainfalls with the same duration. For example, the solid purple
538 line with purple circle markers (representing 2 year-3 hours rainfall scenario) overlaps the red
539 dashed line with the red circle markers (representing 5 year-3 hours rainfall scenario). However,
540 there are still some differences between scenarios with different rainfall duration. Notably, the
541 intra-cluster distance increases as the rainfall duration decreases (the distance for the ‘3hrs’
542 duration rainfall is the largest, followed by the ‘12hrs’ cases, and then the ‘48hrs’ scenarios). As a
543 metric for clustering performance, intra-cluster distance is therefore useful in determining how
544 well these algorithms group the water depth time-series. These results suggest that the K-means
545 and Spectral Clustering algorithms work best with longer duration rainfalls. This suggests that the
546 longer duration rainfall results in greater similarity in the flow at different junctions. This, coupled
547 with the larger set of observations from a longer period, results in better formed individual clusters.
548 Shende and Chau (2019) have shown that these cluster methods work optimally when trained on
549 massive datasets, which is supported by our results herein.

550



551

552 Figure.9 Cluster Intra-distance for comparing the effects of rainfall duration and return period on the performance of
553 K-means and Spectral model (elbow point is the cross between the red dash-line and curves) under 6 synthetic rainfall
554 scenarios ('yr' represents year while 'hrs' stands for hours).

555 5. Discussions

556 In this study, we used unsupervised machine learning algorithms to group simulated time-series
557 water depth of urban drainage systems under six synthetic rainfalls and two measured storms. We
558 applied three different algorithms (K-means clustering, Agglomerative clustering, and Spectral
559 clustering), and evaluated the results using three indices (Silhouette Coefficient, Calinski-Harabasz
560 Index, and Davies-Bouldin Index). These results provide a better theoretical understanding of the
561 different methods, how to use them with these data, and which metrics are suitable for assessing
562 the cluster solutions. We also demonstrate how the characteristics of the dataset (notably length
563 and magnitude) influence the number of clusters. This information should help facilitate the

564 detection of urban flooding events using water depth datasets in real drainage networks (Chang *et*
565 *al.* 2010; Guo *et al.* 2018).

566 Previous cluster-based studies have mainly focused on detecting pressure, demand, pipe burst,
567 infrastructure damage, and illicit intrusion in water distribution systems (Perelman and Ostfeld
568 2012; Sambito *et al.* 2019; Wu and Liu 2020; Xing and Sela 2019). In the clustering analysis here,
569 the features, such as the length of time-series water depth from UDSs, are found to be negatively
570 correlated with the number of clusters. This finding has been validated by the dendrogram cut-off
571 points in designed rainfalls and also by the cluster center mapping based on real storm events. The
572 similar results between the artificial (noise-free) and practical (noise-polluted) scenario infer that
573 modeling duration (data length) overwhelms the event exceedance probability (data magnitude) in
574 the cluster number identification, which agrees with the findings from Wu *et al.* 2016. Increasing
575 the number of clusters often results in many more errors. One extreme case is that the zero error
576 happens when each data point is equal to every cluster. Intuitively, the choice of the best number
577 of clusters can be interpreted into a trade-off between maximum compression of the data with a
578 single cluster and maximum accuracy by assigning each data point to its cluster (WIKIPEDIA
579 2015).

580 In addition to the cluster number determination, the structure of datasets may also affect the
581 clustering model performance. K-means and Spectral Clustering algorithms are able to robustly
582 group water depth datasets from longer duration rainfall events. However, there is little
583 relationship between algorithm performance and annual exceedance probability. The sharply rising
584 trend (Figure.4 to Figure.6) demonstrates that the CHI is not suitable to identify the best number
585 of clusters in the K-means and Agglomerative Clustering algorithms, but that the SCI and DBI
586 work quite well and give comparable results (Figures 4, 5 and 6). In contrast, the CHI works well

587 in identifying the optimal cluster number with the Spectral Clustering algorithm. This difference
588 reflects the different nature of the algorithms: K-means and Agglomerative Clustering are based
589 on simple dissimilarity measures between observations, whereas the Spectral Clustering is based
590 on a graph representing connectivity. This is because that DBI evaluates intra-cluster similarity
591 among every data point and inter-cluster differences among each group. Similarly, the SCI
592 measures the distance between each data point and the centroid of the cluster it was assigned to.
593 An SCI value close to 1 is always good, and a DBI value close to 0 is also good whatever clustering
594 you are trying to evaluate. However, the CHI is not normalized, and it's difficult to compare two
595 values of the CHI index from different data sets.

596 Although this study has identified some clear differences in the application of cluster analysis,
597 there are several limitations. Firstly, the majority of scenarios used time-series water depth datasets
598 generated by model simulation. As these are smooth and noise-free, the results may not scale to
599 field application. However, we found similarities between the results with the limited set of
600 observed rainfall series used here, notably in the use of the different indices, but tend to result in a
601 smaller number of clusters. Further work should apply these methods to a wider set of observed
602 data if such data becomes available. Secondly, this paper only focuses on clustering model
603 implementation and performance evaluation. Future work will concentrate on the application of
604 these methods, including sensor placement, overflow detection, and flooding monitoring. Since
605 the dendrogram enables the AC algorithm to detect outliers in time-series water depth datasets,
606 this can be used to help guide sensor deployment for observing overflow and flooding forecasting
607 in the field (Panganiban and Cruz 2017). It is planned to consider strengthening the connection
608 between the theoretical results and field application by conducting a clustering analysis to optimize
609 the sensor monitoring network for flooding detection at UDSs.

610 **6. Conclusions**

611 In the age of ‘Smart Stormwater,’ the increased deployment of sensors to monitor flow
612 characteristics is resulting in rapidly accumulating data. It is becoming crucial to understand and
613 promote methods to handle these big datasets to help in flood monitoring and forecasting. This
614 study aims to promote understanding of how clustering analysis facilitates the interpretation of the
615 unlabeled time-series water depth data for flood detection at urban drainage systems. In this work,
616 three indexes, including Silhouette Coefficient Index, Calinski-Harabasz Index, and Davies-
617 Bouldin Index, were used to evaluate the performance of three popular unsupervised clustering
618 analysis models namely K-means clustering, Agglomerative clustering, and Spectral clustering. A
619 real-world urban drainage systems SWMM model was applied to generate the time-series water
620 depth under six rainfall scenarios and two real rainstorms. Four conclusions were drawn below:

621 (1) Silhouette Coefficient Index and Davies-Bouldin Index are suitable metrics to measure the
622 performance of K-means and Agglomerative clustering model when subject to identify the
623 number of clusters for the best performance. However, Calinski-Harabasz Index is found
624 to be more favorable to assess the performance of the Spectral clustering model in grouping
625 time-series water depth datasets.

626 (2) In K-means and Spectral clustering models, the number of the clusters for maximizing
627 model performance is highly related to the dataset length (simulation duration) but is
628 slightly associated with the dataset magnitude. There is a negative correlation between the
629 number of clusters and the length of datasets (modeling timesteps).

630 (3) The short-period water depth data can be well-grouped by the Agglomerative clustering
631 model. In contrast, K-means and Spectral clustering models are more able to handle time-

632 series water depth datasets from long-duration storm scenarios.

633 (4) This research work provides insight into unlabeled hydraulic data-driven techniques by
634 conducting clustering experiments. The outcomes are useful for researchers to select the
635 appropriate clustering model and to choose the corresponding performance metrics for
636 specific case applications.

637

638 **Declarations of interest**

639 None

640

641 **Acknowledgments**

642 We would like to thank the Salt Lake City Department of Public Utilities (SLCDPU) for their
643 efforts in developing the SWMM model. We also show great thanks to Professor Steven Burian
644 and the Student Engineering Association (SAE) of the University of Utah for sharing their relevant
645 files and materials. This research is supported by the Research Assistant Scholarship at the
646 University of Utah.

647

648 **References**

649 Aggarwal, C.C., Zhai, C.X., 2012. A survey of text clustering algorithms, in: Mining Text Data.
650 https://doi.org/10.1007/978-1-4614-3223-4_4

651 Al-Zoubi, M.B., Al Rawi, M., 2008. An efficient approach for computing silhouette coefficients. *Journal of Computer*
652 *Science*. <https://doi.org/10.3844/jcssp.2008.252.255>

653 Aranganayagi, S., Thangavel, K., 2008. Clustering categorical data using silhouette coefficient as a relocating measure,
654 in: *Proceedings - International Conference on Computational Intelligence and Multimedia Applications*,
655 *ICCIMA 2007*. <https://doi.org/10.1109/ICCIMA.2007.127>

656 Bowes, B.D., Sadler, J.M., Morsy, M.M., Behl, M., Goodall, J.L., 2019. Forecasting groundwater table in a flood
657 prone coastal city with long short-term memory and recurrent neural networks. *Water (Switzerland)*.
658 <https://doi.org/10.3390/w11051098>

659 Bro, R., Smilde, A.K., 2014. Principal component analysis. *Analytical Methods*. <https://doi.org/10.1039/c3ay41907j>

660 Caliński, T., Harabasz, J., 1974. A Dendrite Method For Cluster Analysis. *Communications in Statistics*.
661 <https://doi.org/10.1080/03610927408827101>

662 Celebi, M.E., Kingravi, H.A., Vela, P.A., 2013. A comparative study of efficient initialization methods for the k-
663 means clustering algorithm. *Expert Systems with Applications*. <https://doi.org/10.1016/j.eswa.2012.07.021>

664 Chang, L.C., Shen, H.Y., Wang, Y.F., Huang, J.Y., Lin, Y.T., 2010. Clustering-based hybrid inundation model for
665 forecasting flood inundation depths. *Journal of Hydrology*. <https://doi.org/10.1016/j.jhydrol.2010.02.028>

666 Chen, J.R., 2007. Useful clustering outcomes from meaningful time series clustering. *Conferences in Research and*
667 *Practice in Information Technology Series*.

668 Chen, J.R., 2005. Making subsequence time series clustering meaningful, in: *Proceedings - IEEE International*
669 *Conference on Data Mining, ICDM*. <https://doi.org/10.1109/ICDM.2005.91>

670 Cordeiro De Amorim, R., Mirkin, B., 2012. Minkowski metric, feature weighting and anomalous cluster initializing
671 in K-Means clustering. *Pattern Recognition*. <https://doi.org/10.1016/j.patcog.2011.08.012>

672 Danielsson, P.E., 1980. Euclidean distance mapping. *Computer Graphics and Image Processing*.
673 [https://doi.org/10.1016/0146-664X\(80\)90054-4](https://doi.org/10.1016/0146-664X(80)90054-4)

- 674 Davies, D.L., Bouldin, D.W., 1979. A Cluster Separation Measure. *IEEE Transactions on Pattern Analysis and*
675 *Machine Intelligence*. <https://doi.org/10.1109/TPAMI.1979.4766909>
- 676 Diao, K., Farmani, R., Fu, G., Astaraie-Imani, M., Ward, S., Butler, D., 2014. Clustering analysis of water distribution
677 systems: Identifying critical components and community impacts. *Water Science and Technology*.
678 <https://doi.org/10.2166/wst.2014.268>
- 679 Forina, M., Armanino, C., Raggio, V., 2002. Clustering with dendrograms on interpretation variables. *Analytica*
680 *Chimica Acta*. [https://doi.org/10.1016/S0003-2670\(01\)01517-3](https://doi.org/10.1016/S0003-2670(01)01517-3)
- 681 Fotovatikhah, F., Herrera, M., Shamshirband, S., Chau, K.W., Ardabili, S.F., Piran, M.J., 2018. Survey of
682 computational intelligence as basis to big flood management: Challenges, research directions and future work.
683 *Engineering Applications of Computational Fluid Mechanics*. <https://doi.org/10.1080/19942060.2018.1448896>
- 684 Hastie, T., Tibshirani, R., Friedman, J., 2009. *Elements of Statistical Learning 2nd ed., Elements*.
685 <https://doi.org/10.1007/978-0-387-84858-7>
- 686 Henonin, J., Russo, B., Mark, O., Gourbesville, P., 2013. Real-time urban flood forecasting and modelling – a state
687 of the art. *Journal of Hydroinformatics*. <https://doi.org/10.2166/hydro.2013.132>
- 688 Hsu, N.S., Huang, C.L., Wei, C.C., 2013. Intelligent real-time operation of a pumping station for an urban drainage
689 system. *Journal of Hydrology*. <https://doi.org/10.1016/j.jhydrol.2013.02.047>
- 690 Hu, Y., Scavia, D., Kerkez, B., 2018. Are all data useful? Inferring causality to predict flows across sewer and drainage
691 systems using directed information and boosted regression trees. *Water Research* 145, 697–706.
692 <https://doi.org/10.1016/j.watres.2018.09.009>
- 693 Jain, A.K., Murty, M.N., Flynn, P.J., 1999. Data clustering: A review, in: *ACM Computing Surveys*.
694 <https://doi.org/10.1145/331499.331504>
- 695 Kang, O.Y., Lee, S.C., Wasewar, K., Kim, M.J., Liu, H., Oh, T.S., Janghorban, E., Yoo, C.K., 2013. Determination
696 of key sensor locations for non-point pollutant sources management in sewer network. *Korean Journal of*
697 *Chemical Engineering* 30, 20–26. <https://doi.org/10.1007/s11814-012-0108-y>

698 Keogh, E., Lin, J., Truppel, W., 2003. Clustering of time series subsequences is meaningless: Implications for previous
699 and future research. *Proceedings - IEEE International Conference on Data Mining, ICDM* 115–122.
700 <https://doi.org/10.1007/s10115-004-0172-7>

701 Kerkez, B., Gruden, C., Lewis, M., Montestruque, L., Quigley, M., Wong, B., Bedig, A., Kertesz, R., Braun, T.,
702 Cadwalader, O., Poresky, A., Pak, C., 2016. Smarter stormwater systems. *Environmental Science and*
703 *Technology*. <https://doi.org/10.1021/acs.est.5b05870>

704 Koo, D., Piratla, K., Matthews, C.J., 2015. Towards Sustainable Water Supply: Schematic Development of Big Data
705 Collection Using Internet of Things (IoT), in: *Procedia Engineering*.
706 <https://doi.org/10.1016/j.proeng.2015.08.465>

707 Kubat, M., 2017. An Introduction to Machine Learning, *An Introduction to Machine Learning*.
708 <https://doi.org/10.1007/978-3-319-63913-0>

709 Li, J., Yang, X., Sitzenfrei, R., 2020. Rethinking the Framework of Smart Water System: A Review. *Water*
710 (Switzerland). <https://doi.org/10.3390/w12020412>

711 Li, J., Bao, S., Burian, S., 2019a. Real-time data assimilation potential to connect micro-smart water test bed and
712 hydraulic model. *H2Open Journal*. <https://doi.org/10.2166/h2oj.2019.006>

713 Li, J., Tao, T., Kreidler, M., Burian, S., Yan, H., 2019b. Construction Cost-Based Effectiveness Analysis of Green
714 and Grey Infrastructure in Controlling Flood Inundation: A Case Study. *Journal of Water Management*
715 *Modeling*. <https://doi.org/10.14796/jwmm.c466>

716 Lloyd, S.P., 1982. Least Squares Quantization in PCM. *IEEE Transactions on Information Theory*.
717 <https://doi.org/10.1109/TIT.1982.1056489>

718 Maier, H.R., Kapelan, Z., Kasprzyk, J., Kollat, J., Matott, L.S., Cunha, M.C., Dandy, G.C., Gibbs, M.S., Keedwell,
719 E., Marchi, A., Ostfeld, A., Savic, D., Solomatine, D.P., Vrugt, J.A., Zecchin, A.C., Minsker, B.S., Barbour,
720 E.J., Kuczera, G., Pasha, F., Castelletti, A., Giuliani, M., Reed, P.M., 2014. Evolutionary algorithms and other
721 metaheuristics in water resources: Current status, research challenges and future directions. *Environmental*
722 *Modelling and Software*. <https://doi.org/10.1016/j.envsoft.2014.09.013>

723 Maulik, U., Bandyopadhyay, S., 2002. Performance evaluation of some clustering algorithms and validity indices.
724 IEEE Transactions on Pattern Analysis and Machine Intelligence.
725 <https://doi.org/10.1109/TPAMI.2002.1114856>

726 Moazen-zadeh, R., Mohammadi, B., Shamshirband, S., Chau, K.W., 2018. Coupling a firefly algorithm with support
727 vector regression to predict evaporation in northern Iran. Engineering Applications of Computational Fluid
728 Mechanics. <https://doi.org/10.1080/19942060.2018.1482476>

729 Morales, V.M., Mier, J.M., Garcia, M.H., 2017. Innovative modeling framework for combined sewer overflows
730 prediction. Urban Water Journal. <https://doi.org/10.1080/1573062X.2015.1057183>

731 Mosavi, A., Ozturk, P., Chau, K.W., 2018. Flood prediction using machine learning models: Literature review. Water
732 (Switzerland). <https://doi.org/10.3390/w10111536>

733 Mullapudi, A., Kerkez, B., 2018. Autonomous Control of Urban Storm Water Networks Using Reinforcement
734 Learning. <https://doi.org/10.29007/hx4d>

735 Norbiato, D., Borga, M., Degli Esposti, S., Gaume, E., Anquetin, S., 2008. Flash flood warning based on rainfall
736 thresholds and soil moisture conditions: An assessment for gauged and ungauged basins. Journal of Hydrology.
737 <https://doi.org/10.1016/j.jhydrol.2008.08.023>

738 Panganiban, E.B., Cruz, J.C.D., 2017. Rain water level information with flood warning system using flat clustering
739 predictive technique, in: IEEE Region 10 Annual International Conference, Proceedings/TENCON.
740 <https://doi.org/10.1109/TENCON.2017.8227956>

741 Pedregosa, F., Varoquaux, G., Gramfort, A., Michel, V., Thirion, B., Grisel, O., Blondel, M., Prettenhofer, P., Weiss,
742 R., Dubourg, V., Vanderplas, J., Passos, A., Cournapeau, D., Brucher, M., Perrot, M., Duchesnay, É., 2011.
743 Scikit-learn: Machine learning in Python. Journal of Machine Learning Research.

744 Perelman, L., Ostfeld, A., 2012. Water-Distribution Systems Simplifications through Clustering. Journal of Water
745 Resources Planning and Management 138, 218–229. [https://doi.org/10.1061/\(ASCE\)WR.1943-5452.0000173](https://doi.org/10.1061/(ASCE)WR.1943-5452.0000173)

746 Perelman, L., Ostfeld, A., 2011. Topological clustering for water distribution systems analysis. Environmental

747 Modelling and Software 26, 969–972. <https://doi.org/10.1016/j.envsoft.2011.01.006>

748 Petrovic, S., 2006. A Comparison Between the Silhouette Index and the Davies-Bouldin Index in Labelling IDS
749 Clusters. 11th Nordic Workshop on Secure IT-systems.

750 Rodriguez, A., Laio, A., 2014. Clustering by fast search and find of density peaks. Science 344, 1492–1496.
751 <https://doi.org/10.1126/science.1242072>

752 Rokach, L., Maimon, O., 2010. Chapter 15— Clustering methods. The Data Mining and Knowledge Discovery
753 Handbook. https://doi.org/10.1007/0-387-25465-X_15

754 Rossman, 2015. Storm Water Management Model Reference Manual Volume I – Hydrology. Environmental
755 Protection Agency, Office of Research ... I, 235. <https://doi.org/EPA/600/R-15/162> |

756 Sambito, M., Di Cristo, C., Freni, G., Leopardi, A., 2019. Optimal water quality sensor positioning in urban drainage
757 systems for illicit intrusion identification. Journal of Hydroinformatics 1–15.
758 <https://doi.org/10.2166/hydro.2019.036>

759 Sela Perelman, L., Allen, M., Preis, A., Iqbal, M., Whittle, A.J., 2015. Automated sub-zoning of water distribution
760 systems. Environmental Modelling and Software 65, 1–14. <https://doi.org/10.1016/j.envsoft.2014.11.025>

761 Shannon, W.D., 2007. 11 Cluster Analysis. Handbook of Statistics. [https://doi.org/10.1016/S0169-7161\(07\)27011-7](https://doi.org/10.1016/S0169-7161(07)27011-7)

762 Shende, S., Chau, K.W., 2019. Design of water distribution systems using an intelligent simple benchmarking
763 algorithm with respect to cost optimization and computational efficiency. Water Science and Technology: Water
764 Supply. <https://doi.org/10.2166/ws.2019.065>

765 Solomatine, D.P., Ostfeld, A., 2008. Data-driven modelling: Some past experiences and new approaches, in: Journal
766 of Hydroinformatics. <https://doi.org/10.2166/hydro.2008.015>

767 Stanford, M., 2012. Chapter 7 Hierarchical cluster analysis. Statistics in medicine.

768 Suzuki, R., Shimodaira, H., 2013. pvclust : An R package for hierarchical clustering with p-values. Bioinformatics.

769 Tan, P.N., Steinbach, M., Kumar, V., 2005. Cluster Analysis: Basic Concepts and Algorithms, Chapter 8 in

770 Introduction to Data Mining, in: Addison-Wesley. [https://doi.org/10.1016/0022-4405\(81\)90007-8](https://doi.org/10.1016/0022-4405(81)90007-8)

771 Thorndike, R.L., 1953. Who belongs in the family? *Psychometrika*. <https://doi.org/10.1007/BF02289263>

772 Vojinovic, Z., Abbott, M.B., 2017. Twenty-five years of hydroinformatics. *Water* (Switzerland).
773 <https://doi.org/10.3390/w9010059>

774 Von Luxburg, U., 2007. A tutorial on spectral clustering. *Statistics and Computing*. [https://doi.org/10.1007/s11222-](https://doi.org/10.1007/s11222-007-9033-z)
775 [007-9033-z](https://doi.org/10.1007/s11222-007-9033-z)

776 Wang, W.C., Chau, K.W., Cheng, C.T., Qiu, L., 2009. A comparison of performance of several artificial intelligence
777 methods for forecasting monthly discharge time series. *Journal of Hydrology*.
778 <https://doi.org/10.1016/j.jhydrol.2009.06.019>

779 Ward, J.H., 1963. Hierarchical Grouping to Optimize an Objective Function. *Journal of the American Statistical*
780 *Association*. <https://doi.org/10.1080/01621459.1963.10500845>

781 WIKIPEDIA, 2015. Determining the number of clusters in a data set [WWW Document]. URL
782 https://en.wikipedia.org/wiki/Determining_the_number_of_clusters_in_a_data_set (accessed 11.24.19).

783 Wong, B.P., Kerkez, B., 2016. Real-time environmental sensor data: An application to water quality using web
784 services. *Environmental Modelling and Software*. <https://doi.org/10.1016/j.envsoft.2016.07.020>

785 Wu, Y., Liu, S., 2020. Burst Detection by Analyzing Shape Similarity of Time Series Subsequences in District
786 Metering Areas. *Journal of Water Resources Planning and Management*.
787 [https://doi.org/10.1061/\(ASCE\)WR.1943-5452.0001141](https://doi.org/10.1061/(ASCE)WR.1943-5452.0001141)

788 Wu, Y., Liu, S., Wu, X., Liu, Y., Guan, Y., 2016a. Burst detection in district metering areas using a data driven
789 clustering algorithm. *Water Research* 100, 28–37. <https://doi.org/10.1016/j.watres.2016.05.016>

790 Wu, Y., Liu, S., Wu, X., Liu, Y., Guan, Y., 2016b. Burst detection in district metering areas using a data driven
791 clustering algorithm. *Water Research* 100, 28–37. <https://doi.org/10.1016/j.watres.2016.05.016>

792 Xiao, J., Lu, J., Li, X., 2017. Davies Bouldin Index based hierarchical initialization K-means. *Intelligent Data Analysis*.

793 <https://doi.org/10.3233/IDA-163129>

794 Xing, L., Sela, L., 2019. Unsteady pressure patterns discovery from high-frequency sensing in water distribution
795 systems. *Water Research* 158, 291–300. <https://doi.org/10.1016/j.watres.2019.03.051>

796 Xu, D., Tian, Y., 2015. A Comprehensive Survey of Clustering Algorithms. *Annals of Data Science*.
797 <https://doi.org/10.1007/s40745-015-0040-1>

798 Xu, R., Wunsch, D., 2005. Survey of clustering algorithms. *IEEE Transactions on Neural Networks*.
799 <https://doi.org/10.1109/TNN.2005.845141>

800 Yaseen, Z.M., Sulaiman, S.O., Deo, R.C., Chau, K.W., 2019. An enhanced extreme learning machine model for river
801 flow forecasting: State-of-the-art, practical applications in water resource engineering area and future research
802 direction. *Journal of Hydrology*. <https://doi.org/10.1016/j.jhydrol.2018.11.069>

803 Zhang, K., Tsang, I.W., Kwok, J.T., 2008. Improved Nyström low-rank approximation and error analysis, in:
804 Proceedings of the 25th International Conference on Machine Learning.
805 <https://doi.org/10.1145/1390156.1390311>

806 Zhou, X., Tang, Z., Xu, W., Meng, F., Chu, X., Xin, K., Fu, G., 2019. Deep learning identifies accurate burst locations
807 in water distribution networks. *Water Research*. <https://doi.org/10.1016/j.watres.2019.115058>

808